The C-terminal, third conserved motif of the protein activator PACT plays an essential role in the activation of double-stranded-RNA-dependent protein kinase (PKR)

Xu HUANG, Brian HUTCHINS and Rekha C. PATEL[1]

Department of Biological Sciences, University of South Carolina, 700 Sumter Street, Columbia, SC 29208, U.S.A.

One of the key mediators of the antiviral and antiproliferative actions of interferon is double-stranded-RNA-dependent protein kinase (PKR). PKR activity is also involved in the regulation of cell proliferation, apoptosis and signal transduction. We have recently identified PACT, a novel protein activator of PKR, as an important modulator of PKR activity in cells in the absence of viral infection. PACT heterodimerizes with PKR and activates it by direct protein–protein interactions. Endogenous PACT acts as an activator of PKR in response to diverse stress signals, such as serum starvation and peroxide or arsenite treatment, and is therefore a novel, stress-modulated physiological activator of PKR. In this study, we have characterized the functional domains of PACT that are required for PKR activation. Our results have shown that, unlike the N-terminal conserved domains 1 and 2, the third conserved domain of PACT is dispensable for its binding of double-stranded RNA and interaction with PKR. However, a deletion of domain 3 results in a loss of PKR activation ability, in spite of a normal interaction with PKR, thereby indicating that domain 3 plays an essential role in PKR activation. Purified recombinant domain 3 could also activate PKR efficiently *in vitro*. Our results indicate that, although dispensable for PACT's high-affinity interaction with PKR, the third motif is essential for PKR activation. In addition, domain 3 and eukaryotic initiation factor 2α both interact with PKR through the same region within PKR, which we have mapped to lie between amino acid residues 318 and 551.

Key words: apoptosis, double-stranded RNA, interferon, protein kinase.

INTRODUCTION

Interferons (IFNs) are cytokines with antiviral, antiproliferative and immunomodulatory properties, which they exert by inducing the expression of several genes at the transcriptional level [1]. The IFN-induced double-stranded (ds)-RNA-dependent protein kinase (PKR) is a serine/threonine kinase that is responsible for the antiproliferative and antiviral actions of IFN [2,3]. PKR is present at a basal low level in cells, and its expression is induced severalfold by treatment with IFN or virus infection. The kinase activity of PKR remains latent until it is bound to an activator. The best characterized activator of PKR is dsRNA, but certain polyanionic agents such as heparin have also been shown to activate PKR *in vitro* [4]. Upon binding to dsRNA, the ATP-binding site of PKR is unmasked due to a conformational change, and it is autophosphorylated on several sites. The best-studied physiological substrate of PKR activity is the α subunit of eukaryotic initiation factor 2 (eIF2α) [5], and phosphorylation of eIF2α on Ser-51 by PKR leads to a general block in protein synthesis [6]. Upon viral infection of IFN-treated cells, PKR is activated by viral dsRNA, which in turn leads to a block in protein synthesis. Thus PKR plays a central role in the antiviral activity of IFN [7].

In addition, PKR is involved in the regulation of apoptosis [8,9], cell proliferation [10,11], signal transduction [12–14] and differentiation [15,16]. Overexpression or activation of PKR in HeLa [17,18], COS-1 [19], U937 [20,21] and NIH 3T3 [19] cells leads to apoptosis. Mouse embryo fibroblasts (MEFs) from PKR knock-out mice are resistant to the apoptotic cell death in response to dsRNA, tumour necrosis factor-α (TNF-α) and lipopolysaccharide that has been attributed in part to the defective activation of nuclear factor κB [22–24]. Expression of a trans-dominant negative, catalytically inactive mutant of PKR (K296R) or overexpression of p58, a cellular inhibitor of PKR, in NIH 3T3 cells protects them from apoptosis in response to TNF-α, dsRNA or serum deprivation [19,25]. PKR is also involved in apoptosis induced by encephalomyocarditis infection [26]. Furthermore, forced expression of a non-phosphorylatable S51A mutant of eIF2α partially protected cells from TNF-α-induced apoptosis [19]. Overexpression of PKR in a tetracycline-inducible manner and subsequent activation by dsRNA resulted in apoptosis due to expression of members of TNF receptor family, Fas and pro-apoptotic Bax [25]. Expression of Bcl-2 has been shown to block PKR-induced apoptosis [27]. Mechanisms of PKR-induced apoptosis also include p53-mediated death signalling [21,28]. Although PKR activity has been shown to contribute to several signal transduction pathways, the exact mechanism by which PKR contributes to these pathways is not clear at present. PKR has been shown to affect protein kinases such as p38, JNK (c-Jun N-terminal kinase) [29] and IKK (IκB kinase) [30], and downstream target transcription factors such as p53 [21,28], nuclear factor κB [9], IRF-1 (IFN regulatory

Abbreviations used: DAPI, 4,6-diamidino-2-phenylindole; ds, double-stranded; DTT, dithiothreitol; GFP, green fluorescent protein; eIF2, eukaryotic initiation factor 2; IFN, interferon; MEF, mouse embryo fibroblast; PACT, protein activator of PKR; PKR, double-stranded-RNA-dependent protein kinase; TNF-α, tumour necrosis factor-α; TRBP, TAR (*trans*-activation-responsive RNA of HIV-1) RNA-binding protein.

[1] To whom correspondence should be addressed (e-mail patelr@sc.edu).

factor-1) [13], STATs (signal transduction and activators of transcription) 1 and 3 [14] and ATF (activating transcription factor) [31].

PACT (protein activator of PKR) is a newly identified protein which heterodimerizes with PKR and activates it in the absence of dsRNA [32]. Like PKR, PACT is expressed in most cell types at very low abundance, and its forced overexpression in mammalian cells causes PKR activation, leading to eIF2α phosphorylation and apoptosis [33]. In yeast, co-expression of PACT with PKR enhances the anti-growth effect of PKR [32]. The mouse homologue of PACT (RAX) has been shown to regulate PKR activation in response to interleukin-3 deprivation or stress signals [34]. We have shown recently that exposure of cells to stress signals results in the rapid phosphorylation of endogenous PACT, followed by its enhanced association with PKR, which leads in turn to activation of PKR [33]. Thus the downstream effects of PACT-induced PKR activation include eIF2α phosphorylation and apoptosis.

PACT belongs to an evolutionarily conserved family of RNA-binding proteins with more than 100 members, found in organisms from *Escherichia coli* to human, some of which have a known function [35]. Many of these proteins contain more than one copy of a conserved motif that is involved in binding highly structured RNAs with no apparent sequence specificity. PACT contains three copies of this motif, of which the N-terminal two copies are very well conserved and the C-terminal third copy is less well conserved. The third copy lacks some of the crucial basic residues known to be important for binding of dsRNA. PKR also belongs to this family of proteins, and has two copies of the conserved dsRNA-binding motif. Our previous results have shown not only that these motifs are important for PKR's dsRNA-binding activity, but also that they mediate protein–protein interaction and are involved in the dimerization of PKR [36–41]. The interaction of PACT with PKR is also mediated through these two motifs in PKR [32]. In the present paper, we have characterized the domains of PACT that are required for its PKR activation potential. Our results indicate an essential role for domain 3 of PACT in PKR activation, and a requirement for domains 1 and 2 in high-affinity interactions with PKR. Domain 3 was found to interact weakly with the C-terminal region of PKR, which overlaps with its eIF2α interaction domain. Thus PACT's three conserved dsRNA-binding/dimerization domains serve distinct functions with regard to PKR activation.

EXPERIMENTAL

Construction of PACT deletion mutants

The various deletion constructs of PACT were made by using the appropriate primers for PCR amplification of the corresponding regions from the PACT/BSIIKS$^+$ construct described previously [32]. The primers used were: M1 sense, 5′ GCTCTAGACATATGGAACCAGGGAAAACACCGATTC 3′; M1 antisense, 5′ GGGGATCCTTATGCATTGGCTTTCAAAATG 3′; M2 sense, 5′ GCTCTAGACATATGGAACCAAAGAACCAGCTTAATC 3′; M2 antisense, 5′ GGGGATCCTTAAGAAATATTACTAAATTTGG 3′; M3 sense, 5′ GCTCTAGACATATGGAACCAAATACAGATTACATCC 3′; M3 antisense, 5′ GGGGATCCTTATAAATACTGCAAAGCATTG 3′. The PCR products were subcloned into pGEMT-Easy vector (Promega). Once the sequence of each deletion construct had been verified, each of the mutants was subcloned into the BSIIKS$^+$ (Stratagene) vector at *Xba*I and *Bam*HI sites. The primer design for PCR was such that the upstream primer included an *Xba*I site followed by an *Nde*I site (the ATG start codon was part of this *Nde*I site) before beginning the PACT sequence, and the downstream primer contained the stop codon inserted right after the end of the PACT sequence followed by a *Bam*HI site. This allowed for the insertion of an oligonucleotide encoding the Flag tag between the *Xba*I and *Nde*I sites to generate Flag-tagged proteins, and also for subcloning into the pET15b vector at *Nde*I–*Bam*HI sites for expression of PACT mutants in *E. coli*. The mammalian expression constructs were generated by subcloning the Flag-tagged versions of deletion mutants in the pCB6$^+$ eukaryotic expression vector between *Xba*I and *Bam*HI sites.

The chimaeric construct T12P3 was created by PCR amplification of the region coding for the C-terminal 117 residues of PACT using the upstream primer 5′ GCCCCGGGAGAACCACATTTCTTTAAC 3′ and the downstream primer 5′ GCAAGCTTTTACTTTCTTTCTGCTATTATC 3′. The resulting PCR product was cloned into the TRBP [TAR (*trans*-activation-responsive RNA of HIV-1) RNA-binding protein]/BSIIKS$^+$ construct using the *Sma*I site within the TRBP coding region and a *Hin*dIII site in the polylinker region of BSIIKS$^+$. This resulted in substituting the C-terminal region of TRBP with that of PACT. The construct codes for a chimaeric protein that contains the N-terminal 211 residues of TRBP and the C-terminal 177 residues of PACT.

The Δ318 mutant of PKR was created by ligating the *Ssp*I–*Bam*HI restriction fragment to *Sma*I–*Bam*HI-digested pGEM3-9T vector. This results in a construct that codes for residues 318–551 of PKR when translated *in vitro* using the T7 TNT system (Promega).

Expression and purification of PACT deletion mutants

The PACT deletion mutants were subcloned into pET15b (Novagen) to generate an in-frame fusion of PACT sequences with a histidine tag. The expression host BL21(DE3) was transformed with these constructs. The bacteria were grown overnight in Luria broth and harvested by centrifugation at 5000 ***g*** for 10 min at 25 °C. The cell pellet was suspended in three times the initial culture volume of fresh Luria broth, and isopropyl β-D-thiogalactoside was added at a final concentration of 2 mM. The culture was incubated at 37 °C with vigorous shaking for 2–3 h, at which point the cells were harvested. The cell pellet from 500 ml of culture typically was suspended in 10 ml of binding buffer (5 mM imidazole, 200 mM NaCl, 20 mM Tris/HCl, pH 7.9, 0.1 % Nonidet P-40) and sonicated at a high setting for five 30 s pulses on ice. The homogenate was centrifuged at 12000 ***g*** for 30 min. The pellet was resuspended in 25 ml of the same buffer and pelleted again at 12000 ***g*** for 30 min. The pellet was then resuspended in 10 ml of denaturing buffer (6 M urea, 5 mM imidazole, 200 mM NaCl, 20 mM Tris/HCl, pH 7.9, 0.1 % Nonidet P-40), followed by incubation on ice for 1 h to dissolve the proteins completely. The insoluble material was removed by centrifugation at 30000 ***g*** for 30 min. The supernatant was mixed with 2 ml of Ni-charged His-bind resin (Novagen). The mixture was incubated at 4 °C for 30 min on a slowly rotating shaker. After binding, the resin was washed with 4×50 ml of denaturing buffer and with 6×50 ml of wash buffer (6 M urea, 60 mM imidazole, 200 mM NaCl, 20 mM Tris/HCl, pH 7.9, 0.1 % Nonidet P-40). The washed resin was packed into a column, and His–PACT was eluted with 25 ml of strip buffer (6 M urea, 100 mM EDTA, 200 mM NaCl, 20 mM Tris/HCl, pH 7.5). The eluted protein was dialysed against 2 litres of buffer at 4 °C in four steps of decreasing urea concentrations (4, 2, 1 and 0.5 M, and finally no urea). The refolded proteins were then concentrated to approx. 400 mg/ml using Centriprep

concentrators. The purity and yield of the proteins was ascertained by SDS/PAGE on 12% (for M1M2 and T12P3 proteins) or 18% (M1, M2 and M3 proteins) gels. The exact concentration of proteins was determined by using BSA as a standard.

dsRNA-binding assays

The *in vitro* translated, ^{35}S-labelled PACT deletion proteins were synthesized using the TNT T7 coupled reticulocyte lysate system from Promega. The dsRNA-binding activity was measured using a poly(I) · poly(C)–agarose binding assay. A 4 μl aliquot of the translation products was diluted with 25 μl of binding buffer [20 mM Tris/HCl, pH 7.5, 0.3 M NaCl, 5 mM $MgCl_2$, 1 mM dithiothreitol (DTT), 0.1 mM PMSF, 0.5% Igepal, 10% glycerol] were mixed with 25 μl of poly(I) · poly(C)–agarose (Pharmacia) beads and incubated at 30 °C for 30 min with intermittent shaking. The beads were then washed with 4 × 500 μl of binding buffer. The proteins bound to the beads after washing were analysed by SDS/PAGE followed by fluorography.

PKR–PACT interaction assays

In vitro translated, ^{35}S-labelled PKR and Flag-epitope-tagged PACT protein or its deletion mutants were co-translated using the TnT T7 coupled reticulocyte system from Promega. A 5 μl aliquot of the *in vitro* translated ^{35}S-labelled proteins was incubated with 20 μl of anti-Flag–agarose (Sigma) in 200 μl of immunoprecipitation buffer (20 mM Tris/HCl, pH 7.5, 100 mM KCl, 1 mM EDTA, 1 mM DTT, 100 units/ml aprotinin, 0.2 mM PMSF, 20% glycerol, 1% Triton X-100) at 4 °C for 30 min on a rotating wheel. The beads were washed in 500 μl of immunoprecipitation buffer four times and the washed beads were then boiled in 2 × Laemmli buffer (150 mM Tris/HCl, pH 6.8, 5% SDS, 5% β-mercaptoethanol, 20% glycerol) for 2 min, and eluted proteins were analysed by SDS/PAGE on a 12% gel. Fluorography was performed at −80 °C with intensifying screens. For analysing the interactions between the M3 deletion construct and PKR at low salt concentrations, the same immunoprecipitation buffer was used, except that the KCl concentration was reduced to 50 mM.

For analysing interactions between purified eIF2, PKR and M3 proteins, the same assay was used with minor modifications. A 50 ng sample of pure recombinant hexahistidine-tagged PKR protein was incubated with 50 ng of purified eIF2 and increasing quantities of recombinant hexahistidine-tagged M3 protein (25–100 ng) in 20 μl of immunoprecipitation buffer containing 50 mM KCl at 4 °C for 30 min on a rotating wheel. The beads were washed in 3 × 200 μl of immunoprecipitation buffer and the washed beads were then boiled in 2 × Laemmli buffer for 2 min, and eluted proteins were analysed by SDS/PAGE on a 12% gel followed by Western blot analysis with anti-PKR (Ribogene; 71/10), anti-eIF2α (Santa Cruz; polyclonal) and anti-His (Santa Cruz; monoclonal) probes.

Translation inhibition assays

The translation-inhibiting activity of PACT and its deletion mutants was tested using a translation inhibition assay as described previously [32]. In this assay, the effect of co-transfection with an effector plasmid on translation of a reporter such as luciferase is tested. MEFs were transfected in six-well plates in triplicate with 800 ng of pGL2-luciferase reporter plasmid and 200 ng of effector plasmid (expression constructs of various deletion mutants of PACT) DNAs using the LIPOFECTAMINE™ (Life Technologies) reagent. At 24 h after transfection, the cells were treated with 100 units/ml IFNβ. Cells were harvested 48 h after transfection and assayed for luciferase activity.

Apoptosis assays

Cells were grown to 50% confluency in six-well plates and co-transfected with 200 ng of the indicated effector and 800 ng of pEGFPC1 (Clontech) plasmid using the LIPOFECTAMINE™ reagent. The cells were observed for green fluorescent protein (GFP) fluorescence 24 h after transfection using an inverted fluorescence microscope, and were then treated with 10 μM sodium arsenite. At 12 h after this treatment, at least 300 fluorescent (GFP-positive) cells were counted as alive or dead, based on their morphology. The cells showing a normal flat morphology were scored as alive, and cells showing cell shrinkage, membrane blebbing, rounded morphology, chromatin condensation or partial detachment from the plate were counted as dead. The percentage of apoptotic cells was calculated using the formula:

$$\text{Apoptosis (\%)} = (\text{fluorescent dead cells/total fluorescent cells}) \times 100$$

For nuclear condensation assays, cells were grown and transfected on coverslips. At 36 h post-transfection, the cells were washed twice with PBS and fixed in acetone/methanol (1:1, v/v) for 1 min, and the coverslips were mounted in Vectashield (Vector Laboratories) mounting medium containing DAPI (4,6-diamidino-2-phenylindole).

Western blot analysis

At 24 or 36 h after transfection, the cell extracts were prepared and Western blot analysis was performed as described previously [32] using the antibodies indicated.

PKR activity assay

PKR activity assays were performed as described previously [30] using an anti-PKR monoclonal antibody (Ribogene; 71/10). HeLa M cells were maintained in Dulbecco's modified Eagle's medium containing 10% (v/v) fetal calf serum. The cells were harvested when they were at 70% confluency. Cells were washed in ice-cold PBS and packed by centrifugation at 600 ***g*** for 5 min. They were lysed by addition of an equal volume of lysis buffer (20 mM Tris/HCl, pH 7.5, 5 mM $MgCl_2$, 50 mM KCl, 400 mM NaCl, 2 mM DTT, 1% Triton X-100, 100 units/ml aprotinin, 0.2 mM PMSF, 20% glycerol). The lysates were centrifuged at 10000 ***g*** for 5 min and the supernatants were assayed for PKR activity. A 100 μg aliquot of total protein was immunoprecipitated using anti-PKR monoclonal antibody (71/10) in high-salt buffer (20 mM Tris/HCl, pH 7.5, 50 mM KCl, 400 mM NaCl, 1 mM EDTA, 1 mM DTT, 100 units/ml aprotinin, 0.2 mM PMSF, 20% glycerol, 1% Triton X-100) at 4 °C for 30 min on a rotating wheel. Then 10 μl of Protein A–Sepharose slurry was added and incubation was carried out for a further 1 h. The Protein A–Sepharose beads were washed four times in 500 μl of high-salt buffer and twice in activity buffer (20 mM Tris/HCl, pH 7.5, 50 mM KCl, 2 mM $MgCl_2$, 2 mM $MnCl_2$, 100 units/ml aprotinin, 0.1 mM PMSF, 5% glycerol). The PKR assay was performed with PKR still attached to the beads in activity buffer containing 250 ng of purified eIF2 (kindly provided by Dr William Merrick, Case Western Reserve University, Cleveland, OH, U.S.A.), 0.1 mM ATP and 1 μCi of [γ-^{32}P]ATP at 30 °C for 10 min. The standard activator of the enzyme was 0.1 μg/ml poly(I) · poly(C) or 0.116 pmol of pure PACT protein.

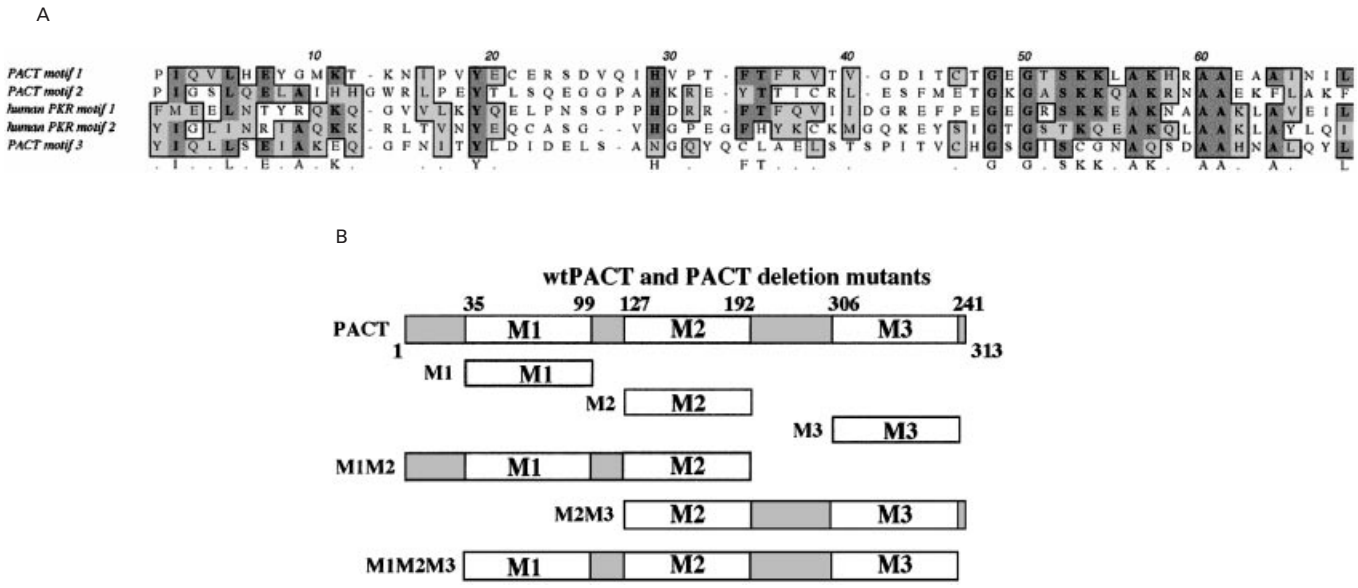

Figure 1 (A) Alignment of conserved dsRNA-binding motifs of PACT and PKR, and (B) schematic representation of the deletion constructs of PACT

(**A**) The three conserved motifs of PACT (M1–M3) are aligned with the two conserved motifs of PKR. Darkly shaded residues indicate presence in at least three of the motifs, and lightly shaded residues indicate conservative changes from the consensus. The consensus is shown below the alignments. Note that motif M3 of PACT is the least similar among the five motifs and lacks the crucial lysine residues at positions 53, 54 and 57 required for binding of dsRNA. (**B**) The wild-type (wt) PACT protein is shown on the top. The numbers indicate amino acid positions, and are shown to depict the starting and ending points of the three motifs. White boxes indicate the conserved dsRNA-binding motifs, and grey boxes represent the linker sequences between the conserved motifs. The sizes of the constructs are drawn to scale.

Purified PACT deletion proteins in amounts varying from 0.05 to 1 pmol were added to test their effect on PKR activity. Labelled proteins were analysed by SDS/PAGE on a 12 % gel followed by autoradiography.

RESULTS

Motif M3 has no dsRNA-binding activity

Both PKR and PACT belong to the family of RNA-binding proteins that contain one or more copies of a conserved dsRNA-binding motif [35,42]. PKR contains two copies and PACT contains three copies of this motif. An alignment of the conserved motifs is shown in Figure 1(A). The two motifs of PKR and motifs M1 and M2 of PACT are very similar to each other and retain conserved residues at key locations within the motif, as also seen by comparison with the consensus sequence shown at the bottom of Figure 1(A). On the other hand, motif M3 of PACT is less similar, and lacks conservation of the residues crucial for dsRNA binding.

To test the contribution of the three conserved motifs of PACT to its dsRNA-binding activity, several deletion constructs of PACT were generated, as shown in Figure 1(B). The dsRNA-binding activities of the resulting deletion products were tested using a poly(I) · poly(C)–agarose binding assay. We tested each individual motif and three combinations of them. As shown in Figure 2, wild-type PACT bound poly(I) · poly(C)–agarose with high efficiency; 73 % of the input counts were bound to the beads. Single motifs M1 and M2 bound to poly(I) · poly(C)–agarose with reduced efficiency (20 % and 23 % binding respectively) compared with the full-length PACT protein, as expected due to the co-operative manner in which these motifs are known to function [43,44]. Motif M3, however, showed no dsRNA-binding activity. The M1M2 protein showed dsRNA-binding activity that was comparable with that of wild-type PACT, as 89 % of input counts bound to the beads, confirming that the two motifs M1 and M2 act in a co-operative manner. The M2M3 protein showed only 18 % binding to the beads, which is significantly lower than that of either full-length PACT or M1M2, but similar to the dsRNA-binding activity of motif M2 alone. These results are in agreement with the observation that motif M3 does not contribute to the dsRNA-binding activity of PACT, and therefore probably does not act in a co-operative manner with M2 to enhance the dsRNA-binding affinity. The M1M2M3 protein also seemed to have reduced dsRNA-binding activity compared with full-length PACT and M1M2, as only 41 % of this protein was retained on the beads. This indicates that the M3 motif, when present, acts to reduce the binding activity of the other motifs present in the protein. When linked to the M2 motif, M3 reduces its binding affinity from 23 % to 18 %, and when linked to M1M2 it reduces dsRNA binding from 89 % to 41 %. The reason for this and its biological significance remain to be explored.

Motif M3 is dispensable for interaction with PKR

Since our previous results have demonstrated that the two copies of conserved motifs in PKR contribute towards its interaction with PACT, we also tested the ability of deletion mutants to co-immunoprecipitate PKR. Each of the deletion mutants was expressed as a Flag-epitope-tagged, [^{35}S]methionine-labelled protein by co-translation with untagged PKR. As seen in Figure 3 (lanes 1 and 2), immunoprecipitation of PKR alone with Flag-antibody–agarose did not pull down any PKR, indicating the absence of any non-specific background binding. Both PACT and M1M2 proteins could interact with and co-immunoprecipitate PKR (Figure 3, lanes 4 and 6, arrowheads). These results indicate that deletion of motif M3 does not affect the ability of PACT to interact with PKR, and that the

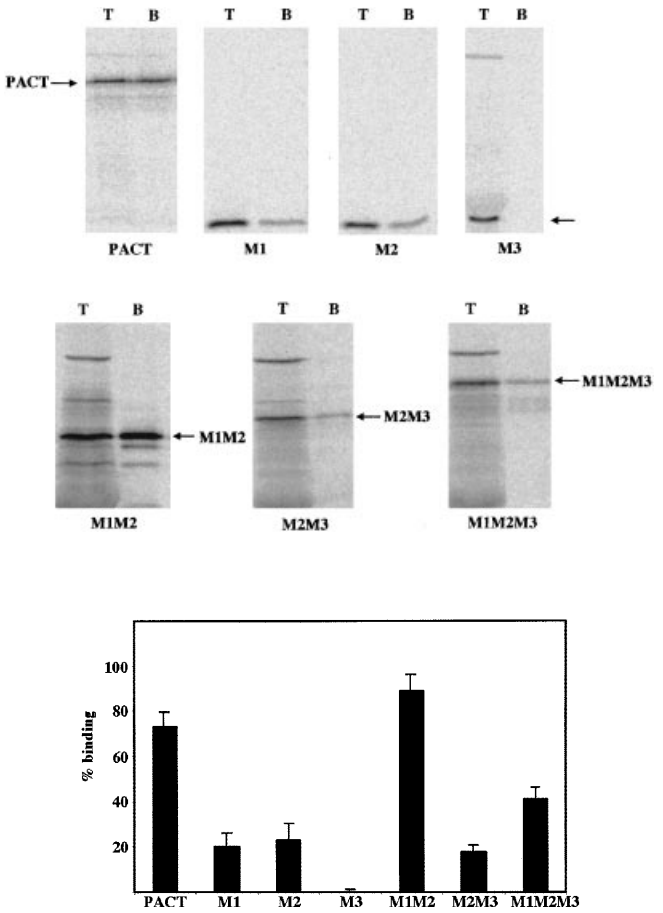

Figure 2 dsRNA-binding activity of deletion constructs of PACT

[^{35}S]Methionine-labelled proteins encoded by various deletion mutants were synthesized by *in vitro* translation using the T7 TNT system. Portions of 5 μl of the reticulocyte lysates were used to assay for poly(I) · poly(C)–agarose binding activity. In the upper panels, lanes labelled T represent 2 μl of total proteins from the lysate, and lanes labelled B represent proteins remaining bound to poly(I) · poly(C)–agarose beads after washing. The names of the deletion mutants are indicated below the panels and the positions of the respective bands are indicated by arrows. Percentage binding to poly(I) · poly(C)–agarose beads was calculated by Phosphorimager analysis (bottom panel). The total input counts and the counts bound to the beads were measured in the corresponding bands, and percentage binding was calculated to represent the percentage of input counts bound to the beads. The error bars indicate S.D.

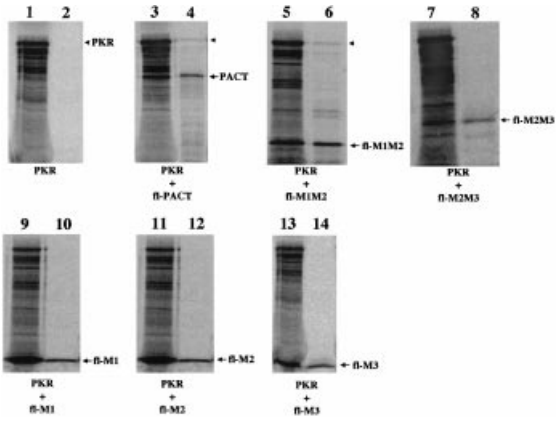

Figure 3 PKR-interaction activity of the deletion constructs of PACT

The Flag (fl)-epitope-tagged, [^{35}S]methionine-labelled proteins encoded by various deletion mutants and wild-type PACT were synthesized by co-translation with untagged wild-type PKR protein using the T7 TNT system. Portions of 5 μl of the reticulocyte lysates were used for co-immunoprecipitation assay using (anti-Flag antibody)–agarose. Odd-numbered lanes contain 2 μl of total proteins from the lysate, and even-numbered lanes contain co-immunoprecipitated proteins remaining bound to the beads after washing. The names of the deletion mutants that were co-translated with PKR are indicated at the bottom of the panels, and the positions of the respective bands are indicated by arrows. The co-immunoprecipitated PKR bands are indicated by arrowheads where seen.

interaction with PKR is mediated primarily through motifs M1 and M2. M2M3 protein was not able to pull down any PKR in the co-immunoprecipitation assays (Figure 3, lane 8), indicating that both the M1 and M2 motifs of PACT are required for the interaction with PKR. However, when the co-immunoprecipitation assays were performed at 50 mM salt, we did observe a weak interaction of M2M3 with PKR (results not shown). None of the individual motifs was able to pull down PKR in our co-immunoprecipitation assays (Figure 3, lanes 10, 12 and 14), thereby indicating that a single motif is not capable of high-affinity interaction with PKR. These results show that, at 200 mM salt, the interaction between PACT and PKR is mediated mainly through motifs M1 and M2, and that motif M3 is dispensable for the interaction. The *in vitro* interaction between PACT and PKR is relatively weak, since only a fraction of the PKR present in the reaction can be co-immunoprecipitated. Our previous *in vivo* results have shown that the PACT–PKR interaction is significantly strengthened by phosphorylation of PACT in response to stress signals [33]. Due to the absence of such a modification *in vitro*, the PACT–PKR interaction is expected to be a low-affinity interaction, as seen in Figure 3.

Motif M3 plays an essential role in PKR activation *in vivo*

We have shown previously that transient overexpression of PACT leads to PKR activation and causes eIF2α phosphorylation in mammalian cells [32]. This can be measured by assaying the expression of a co-transfected reporter gene such as luciferase [32]. This *in vivo* translational repression assay to study PKR activation has been used widely by us and others [39,45–49]. Using this assay, we next determined the ability of the PACT deletion constructs to activate PKR in MEFs. As seen in Figure 4(A), co-transfection with wild-type PKR reduced luciferase activity dramatically, whereas co-transfection with the catalytically inactive K296R PKR mutant increased reporter activity, due to inhibition of endogenous PKR activation. As shown previously, PACT reduced the luciferase activity due to its ability to activate endogenous PKR [32]. Surprisingly, M1M2 increased luciferase activity by more than 2-fold, indicating that this deletion mutant has not only lost its ability to activate PKR, but can also function to inhibit the activation of PKR, acting similarly to a trans-dominant, negative K296R mutant of PKR. The M2M3 protein, on the other hand, resulted in a very marginal reduction of reporter gene activity, which may be due to its ability to interact very weakly with PKR *in vivo*. All three individual motifs were neutral in this assay, neither activating nor inhibiting PKR activity, which is as expected from the results of the interaction assays shown in Figure 3, since none of them showed any interaction with PKR and therefore they are not expected to activate PKR.

We have shown previously that transient overexpression of PACT in mammalian cells leads to apoptosis [32,33]. PACT-overexpressing cells were shown to be more sensitive to stress-induced apoptosis. In order to delineate the domains of PACT

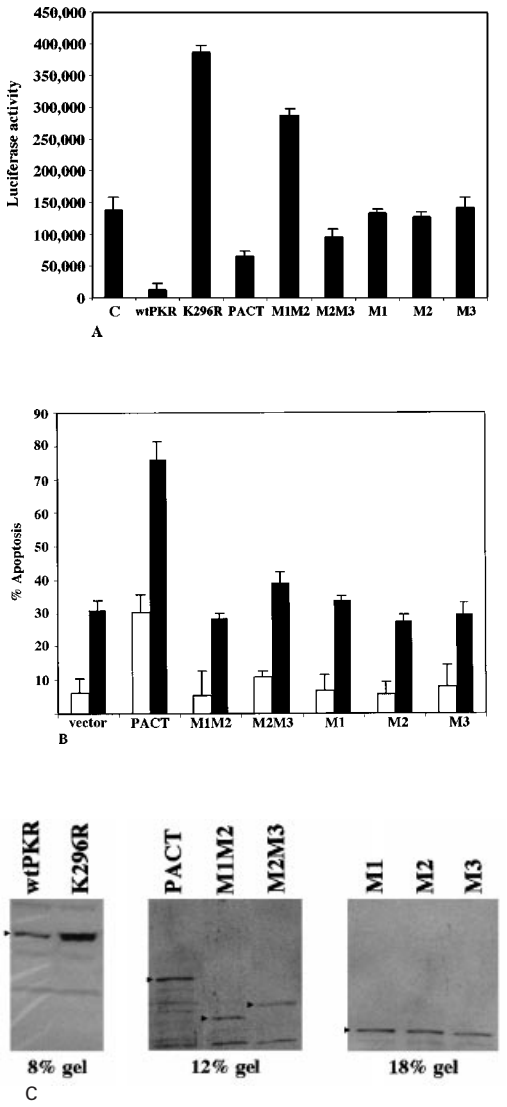

Figure 4 ***In vivo*** **assay of the PKR activation capacity of PACT deletion mutants**

(**A**) Translation inhibition assay. This was performed using MEFs grown in six-well plates. The reporter used was pGL2C (Promega). An 800 ng aliquot of pGL2C was co-transfected using LIPOFECTAMINE™ reagent with 200 ng of the expression constructs for the proteins indicated. At 24 h after transfection, the cells were treated with 100 units/ml IFNβ for 24 h. Luciferase activity was measured in the cell extracts and normalized to the amount of total protein in the extract. All expression constructs were in pCB6$^+$; C indicates the empty-vector (pCB6$^+$) control. Each sample was assayed in triplicate and the data represent means of six samples from two separate experiments. Error bars indicate S.D. (**B**) Ability of PACT mutants to induce apoptosis. NIH 3T3 cells grown on coverslips were co-transfected with pEGFPC1 (Clontech) and Flag–PACT/pCB6$^+$, Flag–M1M2/pCB6$^+$, Flag–M2M3/pCB6$^+$, Flag–M1/pCB6$^+$, Flag–M2/pCB6$^+$, Flag–M3/pCB6$^+$ or pCB6$^+$. At 48 h after transfection, the cells were fixed and mounted in Vectashield mounting medium containing the nuclear stain DAPI. Open bars indicate untreated cells and closed bars represent arsenite-treated cells. For arsenite-treated samples, cells were treated 24 h after transfection with 10 μM sodium arsenite for 12 h. At least 300 GFP-positive cells were counted for each transfected sample and, within this population, the number of cells showing nuclear condensation was noted. The percentage of apoptotic cells among the GFP-expressing population was calculated as follows: percentage apoptosis = (number of cells showing nuclear condensation/total number of cells counted) $\times$ 100. The data represent means of three independent experiments. Error bars represent S.D. (**C**) Western blot analysis of transfected cells. Western blot analysis was performed on the extracts prepared from the transfected cells. The blots were probed with an anti-Flag monoclonal antibody. The presence of Flag-tagged proteins is indicated by arrowheads. The acrylamide content (%) of the SDS/PAGE gels used to analyse the samples is indicated. The labels on the top indicate the transfected construct. wt, wild type.

responsible for apoptosis-inducing activity, we next examined the ability of our mutants to activate an apoptotic pathway in mammalian cells. The expression constructs encoding the deletion mutants were co-transfected with an enhanced GFP expression plasmid and the apoptosis assay was performed in the transfected cells as described previously [33]. The fluorescent cells that showed characteristic signs of apoptosis, such as cytoplasmic shrinkage, membrane blebbing and chromatin condensation, were scored as undergoing apoptosis, and the percentage of apoptotic cells within the transfected population was calculated by counting at least 300 fluorescent cells. As shown in Figure 4(B), in the absence of any stress signal (open bars), PACT co-expression resulted in approx. 30% of cells being apoptotic, compared with only 6% apoptotic cells in the vector control. None of the deletion constructs showed any significant levels of apoptosis above the vector control in the absence of a stress stimulus. Arsenite treatment of the transfected cells (Figure 4B, closed bars) resulted in an increase in the number of apoptotic cells, as reported previously [33]. The vector-transfected samples had $\sim$30% cells undergoing apoptosis after arsenite treatment. PACT-overexpressing cells, however, showed approx. 75% apoptosis, confirming our earlier results that PACT overexpression sensitizes cells to stress signals [33]. None of the deletion constructs showed any significant levels of apoptosis above that in the vector control. Of particular significance are the M2M3 data, where we did not observe any apoptosis. Although this mutant did show some activity in translation inhibition assays (Figure 4A), this low level of PKR activation may not be strong enough to induce the apoptotic pathway. These results confirm further the results of the *in vivo* PKR activation assay that the deletion proteins are unable to activate PKR *in vivo*. Figure 4(C) shows the results of the Western blot analysis performed to confirm the expression of Flag-tagged deletion protein products in transfected cells.

Motif M3 alone can activate PKR *in vitro*

In order to test the ability of deletion mutants to activate/inhibit PKR in a biochemical assay, we also expressed M1, M2 and M3 as hexahistidine-tagged proteins in bacteria and purified them by affinity chromatography on Ni–agarose (results not shown). We purified these proteins under denaturing conditions, and all buffers during purification contained 6 M urea. We have shown previously that, under these conditions, no bacterial RNA co-purifies with the proteins [32]. We are therefore certain that our purified preparations did not contain any dsRNA contaminants. Each of the purified proteins was tested for its ability to activate PKR. Since in our *in vivo* assays none of the individual motifs showed any PKR activation capability, we were expecting to confirm the same by biochemical assays. However, surprisingly, as represented in Figure 5(A), purified M3 could activate PKR efficiently (lanes 2 and 3). Neither M1 nor M2 showed any PKR activation (lanes 4–7). These results suggest that the PKR activation domain of PACT maps to the M3 motif. Another interesting observation was that, although M3 activates PKR, as reflected by increased phosphorylation of the PKR band, eIF2α phosphorylation does not seem to correlate with increased PKR phosphorylation to the same extent. In order to investigate the reason for this discrepancy, we performed a dose–response curve for M3-mediated PKR activation. As shown in Figure 5(B), even as little as 0.05 pmol of M3 could activate PKR efficiently. The phosphorylation of the PKR band was seen to increase in a dose-dependent manner with increasing concentrations of M3. eIF2α phosphorylation showed a definite increase over the control (Figure 5B, lane 1) when activated with

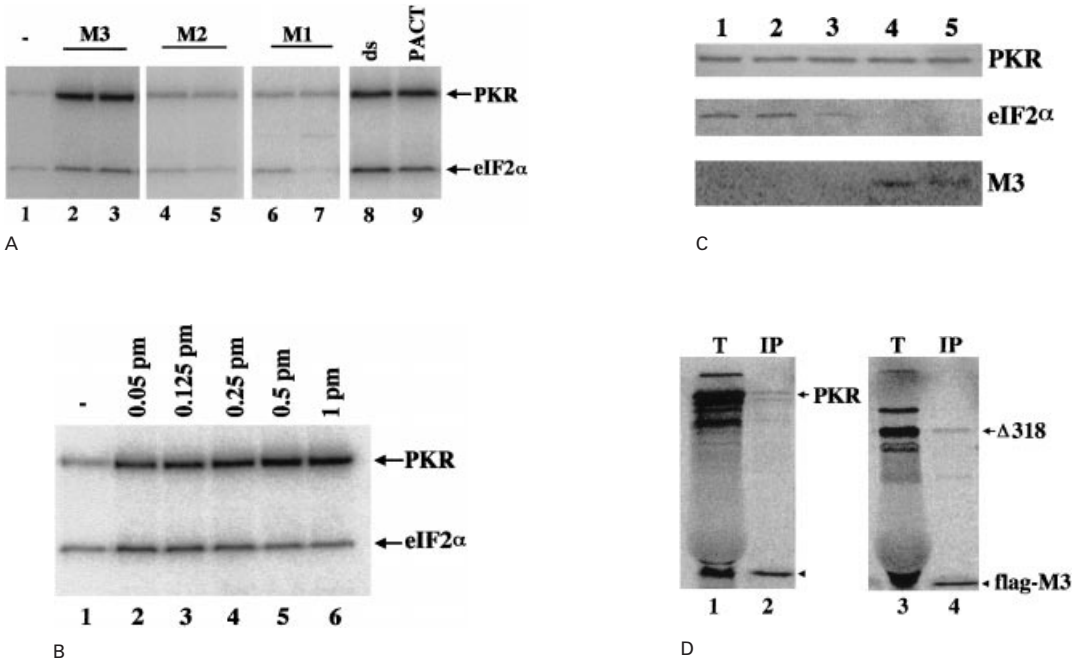

Figure 5 ***In vitro*** **assay of PKR activation capacity of PACT deletion mutants**

(**A**) Only M3 has the capacity to activate PKR. Purified recombinant M1, M2 and M3 proteins were tested for their ability to activate PKR. Lane 1, no activator added; lanes 2 and 3, 0.5 and 1 pmol of pure recombinant M3 respectively; lanes 4 and 5, 0.5 and 1 pmol of pure recombinant M2 respectively; lanes 6 and 7, 0.5 and 1 pmol of pure recombinant M1 respectively; lane 8, 0.1 μg/ml poly(I) · poly(C); lane 8, 0.116 pmol of pure recombinant PACT. The positions of phosphorylated PKR and eIF2α are indicated by arrows. (**B**) M3 can activate PKR in a dose-dependent manner. Purified recombinant M3 protein was added to PKR kinase activity assays. Lane 1, no activator; lanes 2–6 contain the indicated amounts of pure recombinant M3 protein (pm, pmol). The positions of phosphorylated PKR and eIF2α are indicated by arrows. (**C**) M3 and eIF2α interact with PKR through the same domain. Co-immunoprecipitation analysis of PKR and eIF2α was carried out in the presence of increasing amounts of recombinant M3 protein. All lanes have 50 ng of PKR and eIF2 proteins. Lane 1, no M3 added; lane 2, 25 ng; lane 3, 50 ng; lane 4, 75 ng; lane 5, 100 ng. Immunoprecipitation was done with anti-PKR monoclonal antibody 71/10 and Protein A–Sepharose. The immunoprecipitated proteins were separated by SDS/18%-PAGE and transferred to an Immobilon-P^{SQ} membrane for Western blot analysis with anti-eIF2α polyclonal and anti-(hexahistidine tag) monoclonal antibodies. (**D**) The M3 domain interacts with PKR with low affinity at a site downstream of residue 318. The Flag-epitope-tagged, [^{35}S]methionine-labelled protein encoded by Flag–M3/BSIIKS^{+} was synthesized by co-translation with untagged wild-type PKR protein or the Δ318 deletion mutant using the T7 TNT system. Portions of 5 μl of the reticulocyte lysates were used for co-immunoprecipitation assays at low salt concentrations using (anti-Flag antibody)–agarose. Lanes T, 2 μl of total proteins from the lysate; lanes IP, proteins remaining bound to beads after washing. The positions of the respective co-immunoprecipitated bands are indicated by arrows. The Flag-tagged M3 bands are indicated by arrowheads.

0.05, 0.125 or 0.25 pmol of M3 protein (lanes 2–4), but higher concentrations of M3 surprisingly resulted in a decrease in eIF2α phosphorylation (lanes 5 and 6). We reasoned that this could be explained if the M3 motif of PACT was activating PKR by interacting with the same region that eIF2α binds to, thereby precluding it from binding to PKR. At higher concentrations, M3 may preferentially compete out eIF2α binding, thereby reducing the interaction of PKR with its substrate, and this may lead to reduced phosphorylation of eIF2α. To test this hypothesis, we used an *in vitro* interaction assay with purified PKR, eIF2 and M3 proteins. Since we observed no interaction between M3 and PKR at physiological salt concentrations (Figure 3), we performed this co-immunoprecipitation at 50 mM salt (similar to that in PKR activity assays). As seen in Figure 5(C), addition of increasing amounts of M3 protein to the reaction resulted in decreasing amounts of eIF2α co-immunoprecipitating with PKR. This decrease in the interaction of eIF2 with PKR was dependent on increasing M3 concentration; this further supports our hypothesis that PACT and eIF2 may interact with the same domain of PKR.

Another point worth noting is that the interaction between PKR and M3 proteins could be detected in this assay at 50 mM salt. These results are in contrast with the results of co-immunoprecipitation assays done at 200 mM salt (see Figure 3). None of the individual motifs showed any interaction with PKR at physiological salt concentrations used in the co-immunoprecipitation assays. Also, as seen in Figure 4(A), none of the individual motifs was capable of PKR activation *in vivo*. This discrepancy could arise due to the very weak or transient nature of the interaction between M3 and PKR, thereby making it difficult to detect *in vivo* and in co-immunoprecipitation experiments done at high salt concentrations. We therefore decided to investigate these discrepancies further. Since recombinant M3 clearly activates PKR *in vitro* in our biochemical assays, where excess M3 can be added in the reaction, we reasoned that we should be able to detect an interaction between PKR and M3 in co-immunoprecipitation assays if they were performed at low salt (50 mM) conditions similar to the ones used in activity assays. Indeed, the M3 motif showed a positive interaction with PKR under these conditions (Figure 5D, lane 2).

The results in Figure 5(C) indicated that eIF2α and the M3 motif of PACT may interact with the same domain within PKR. In order to test this further, we performed co-immunoprecipitation analysis with PKR deletion mutants to map the region within PKR that interacts with the M3 domain. The eIF2α-interacting domain of PKR has been shown to lie downstream of residue 362 [50,51]. In order to test if the interaction with M3 is also mediated by a C-terminal domain of PKR, we carried out a co-immunoprecipitation assay between M3 and a deletion

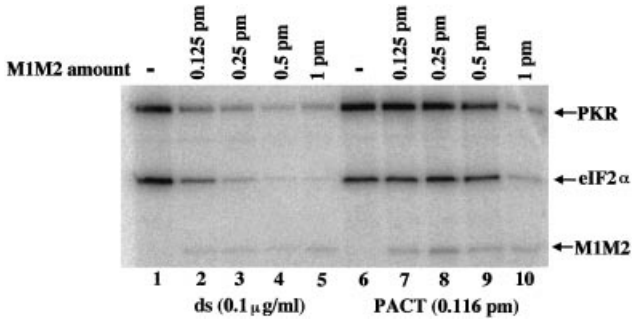

Figure 6 M1M2 mutant protein inhibits PKR activity *in vitro*

PKR immunoprecipitated from HeLa cell extracts was activated by the addition of 0.1 μg/ml of poly(I) · poly(C) (lanes 1–5) or 0.116 pmol of recombinant PACT (lanes 6–10). The effects of addition of increasing amounts of recombinant M1M2 protein were assayed. Lanes 1 and 6, no M1M2 added; lanes 2 and 7, 0.125 pmol (pm); lanes 3 and 8, 0.25 pmol; lanes 4 and 9, 0.5 pmol; lanes 5 and 10, 1 pmol. The positions of phosphorylated PKR and eIF2α are indicated by arrows. The faint band at the bottom represents M1M2 protein, which is also indicated by an arrow.

construct of PKR that lacked the N-terminal 318 residues. As seen in Figure 5(D), lane 4, the Δ318 deletion construct of PKR showed a positive interaction with the M3 domain of PACT. These results support the notion that the M3 and eIF2α interaction domains within PKR may overlap, at least partially.

Deletion of motif M3 converts PACT into an inhibitor of PKR

Deletion of the M3 domain from PACT not only resulted in a loss of its ability to activate PKR, but also converted PACT to act as an inhibitor of PKR (Figure 4A). We tested this further biochemically in PKR activity assays. We expressed M1M2 in bacteria as a hexahistidine-tagged protein and purified it on Ni–agarose by affinity chromatography under denaturing conditions to rule out any co-purification of dsRNA (results not shown). The effect of purified M1M2 protein was tested in kinase activity assays for dsRNA- as well as PACT-induced PKR activation. As seen in Figure 6, addition of as little as 0.125 pmol of pure M1M2 resulted in a dramatic inhibition of dsRNA-mediated PKR activity, and addition of increasing amounts of M1M2 blocked PKR activity further. M1M2 was also able to inhibit PACT-induced PKR activation, although higher quantities of the protein were required for this inhibition. Addition of 1 pmol of purified M1M2 protein could effectively block both dsRNA- and PACT-induced PKR activation. These results clearly demonstrate that M1M2 effectively blocks PKR activation mediated by both dsRNA and PACT, and confirms the results of our *in vivo* translation inhibition assays (Figure 4A).

Motif M3 can confer PKR activation ability on a heterologous protein

Our results have shown that the M3 domain of PACT is both required and sufficient for PKR activation *in vitro*. However, M3 alone was unable to activate PKR *in vivo*, either in translation inhibition assays (Figure 4A) or in apoptosis assays (Figure 4B). We therefore wanted to test if the inability of the M3 domain to activate PKR *in vivo* was due to its extremely weak interaction with PKR, as suggested by our co-immunoprecipitation assays (Figures 3 and 5D). To test this possibility, we constructed a chimaeric protein with two dsRNA-binding/dimerization domains of TRBP joined to M3 of PACT (Figure 7A). TRBP is a protein that is very similar to PACT and also has three copies of the same dsRNA-binding/dimerization domains [36,52–54]. However, unlike PACT, it inhibits PKR activity both *in vivo* and *in vitro* [48,54]. We reasoned that if the M1M2 domains of TRBP could provide a strong interaction with PKR, an M3 domain of PACT fused to it on its C-terminus may be able to activate PKR *in vivo*. We expressed this chimaeric protein, T12P3, in mammalian cells and assayed its ability to activate PKR by a translation inhibition assay. As shown in Figure 7(B), co-transfection with wild-type PKR resulted in a marked reduction in reporter gene activity, and co-transfection with K296R PKR resulted in enhanced reporter gene expression. PACT co-transfection resulted in a reduction in luciferase activity, whereas TRBP co-transfection resulted in an increase in luciferase activity, as expected. Co-transfection with the T12P3 construct resulted in a reduction in luciferase activity, thereby indicating that the third conserved motif of PACT can confer PKR activation ability to a heterologous protein that interacts with PKR. These results suggest that M3 can activate PKR *in vivo* if it is hooked on to a heterologous protein that can interact with high affinity with PKR. In this case, the high-affinity interaction is provided by the two dimerization/dsRNA-binding domains of TRBP. If the translation inhibition caused by T12P3 is mediated by its interaction with PKR, leading to PKR activation, then this effect of T12P3 should be abolished in PKR-null MEFs. As seen in Figure 7(C), co-transfection with wild-type PKR resulted in a marked reduction in luciferase activity, as expected. PACT, K296R or M1M2 did not have any effect on luciferase activity, since there is no endogenous PKR in these cells. Co-transfection with the T12P3 expression construct also had no effect on luciferase activity, thereby confirming that the actions of T12P3 are mediated via activation of PKR. These results confirm that T12P3 acts to repress translation by its ability to interact with and activate PKR, and rule out the participation of any alternative pathways. We confirmed this further by using purified, recombinant T12P3 protein in PKR activity assays *in vitro*. As seen in Figure 7(D), recombinant T12P3 protein could activate PKR efficiently in these assays, in a dose-dependent manner. These results further confirm that the PKR activation domain of PACT resides within motif M3.

DISCUSSION

PACT is a newly identified activator of PKR, and is the only cellular protein known to do this. PACT was cloned as a PKR-interacting protein in a yeast two-hybrid screen by using PKR as a bait protein [32]. PACT belongs to a family of RNA-binding proteins, the members of which have one or multiple copies of an evolutionarily conserved RNA-binding domain [35,42]. PKR itself belongs to this family of proteins and has two copies of this conserved motif. In addition to binding dsRNA, the two copies of the dsRNA-binding motif in PKR have also been shown to mediate its dimerization [36–41]. Thus this motif not only confers RNA-binding ability, but also mediates protein–protein interactions. PACT has three copies of this conserved motif; the two N-terminal copies are very well conserved, but the third, C-terminal, copy is less well conserved and lacks the critical residues involved in the binding of dsRNA (Figure 1A). The interaction of PACT with PKR has been shown by us to be mediated by the two conserved motifs in PKR and is independent of any dsRNA binding [32]. This was shown most conclusively by using point mutants of PKR that were defective in dsRNA binding and therefore could not be activated by dsRNA. Such

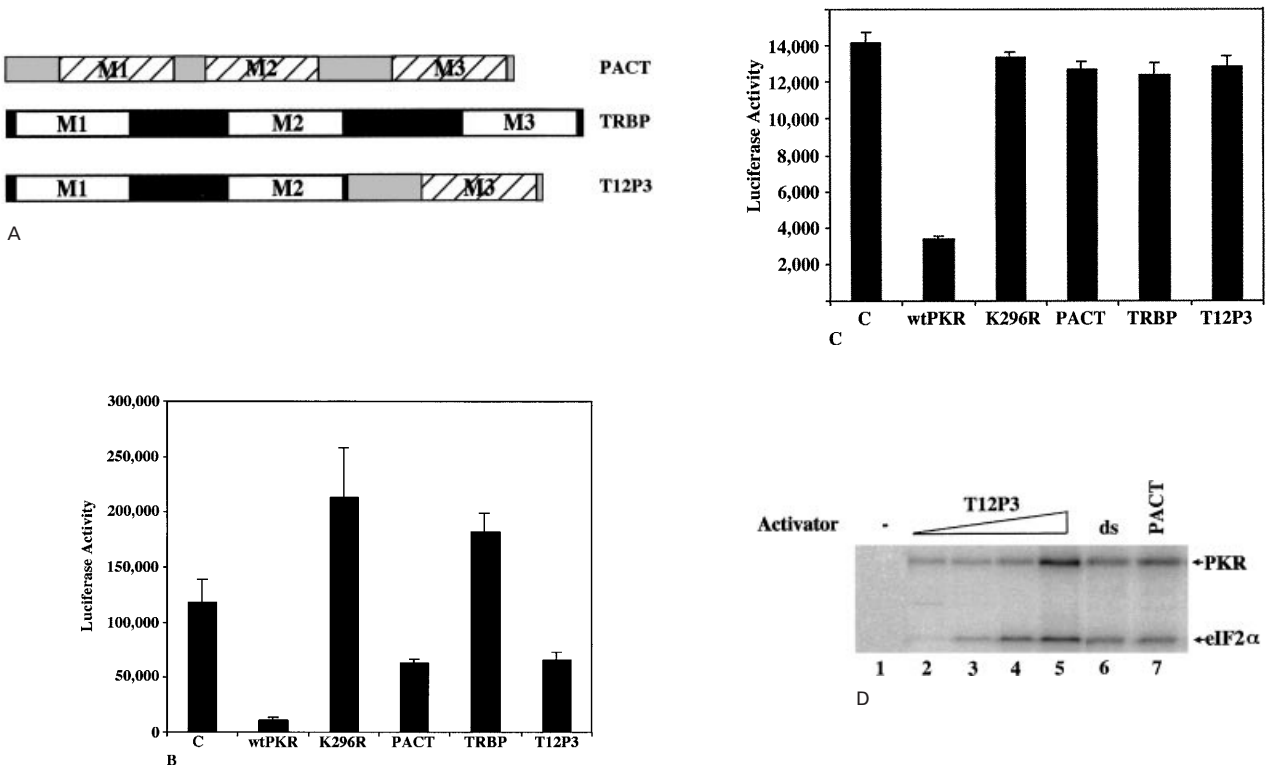

Figure 7 M3 can confer the ability of PKR activation to a heterologous protein

(**A**) Schematic representation of the fusion construct. The white boxes represent conserved motifs M1–M3 of TRBP and the hatched boxes represents motifs M1–M3 from PACT. The lighter grey boxes represent PACT sequences and black boxes represent TRBP sequences. (**B**) *In vivo* assay for PKR activation capacity of the T12P3 protein. The translation inhibition assay was performed in MEFs grown in six-well plates. The reporter used was pGL2C. An 800 ng aliquot of pGL2C was co-transfected using LIPOFECTAMINE™ reagent with 200 ng of the expression construct for the protein indicated. At 24 h after transfection, the cells were treated with 100 units/ml IFNβ for 24 h, and luciferase activity was measured in the cell extracts and normalized to the total protein in the extract. All expression constructs were in pCB6$^+$. C indicates the empty-vector (pCB6$^+$) control. Each sample was assayed in triplicate, and bars represent means of six samples from two separate experiments. Error bars indicate S.D. wt, wild type. (**C**) The inhibitory effect of T12P3 on luciferase translation is abolished in PKR-null MEFs. The translation inhibition assay was performed in the PKR-null MEF cells grown in six-well plates, as described for (**B**). (**D**) Effect of purified chimaeric protein T12P3 on PKR activity. PKR immunoprecipitated from HeLa cell extracts was activated by addition of 0.1 μg/ml poly(I) · poly(C) (ds; lane 6) or 0.116 pmol of recombinant PACT (lane 7). The effect of addition of increasing amounts of recombinant T12P3 protein was assayed. Lane 1, no activator added; lane 2, 0.125 pmol of T12P3; lane 3, 0.25 pmol; lane 4, 0.5 pmol; lane 5, 1 pmol. The positions of phosphorylated PKR and eIF2α are indicated by arrows.

mutants could interact efficiently with PACT and could also be activated by binding to PACT [32]. Recent studies with PACT have indicated that it acts as a protein activator of PKR in cells in the absence of virus infections [33]. Since PKR plays a role in signal transduction to activate different transcription factors in response to various stress signals [9], the identity of PKR's activator in the absence of dsRNA produced by virus infections was unknown until PACT was cloned. Our results have shown that PACT is rapidly phosphorylated in response to stress signals, and associates with PKR, causing its activation and the phosphorylation of eIF2α. Transient overexpression of PACT in mammalian cells renders them more sensitive to apoptosis in response to stress signals [33]. PACT-overexpressing cells were found to be at least 3-fold more sensitive to several diverse stress signals and underwent apoptosis rapidly [33]. PACT has thus emerged as a cellular activator of PKR in the absence of viral infections.

In the present study: we have (1) characterized the domains of PACT that are essential for its interaction with PKR; (2) identified its PKR activation domain; and (3) mapped the site within PKR with which this activation domain of PACT interacts to unmask the kinase activity of PKR. As shown in Figure 1, PACT contains three conserved dsRNA-binding/protein-interaction motifs, represented as M1, M2 and M3. Our results indicate that motifs M1 and M2 can bind to dsRNA individually, but their binding is enhanced if they are present together, suggesting that they act in a co-operative manner. On the other hand, M3 does not show any dsRNA-binding activity, as expected from its sequence, since it lacks the important invariant residues known to be crucial for binding of dsRNA. Similarly, deletion of M3 results in a truncated protein that binds to dsRNA with at least the same affinity as full-length PACT, further indicating that M3 plays no role in PACT's dsRNA-binding activity. Deletion of the M1 motif was seen to result in a protein with weak binding to dsRNA, further supporting the idea that the M3 motif neither participates in binding of dsRNA nor acts in a co-operative manner to enhance M2's dsRNA-binding affinity. Similar to PACT's dsRNA-binding activity, both the M1 and M2 motifs are required for its efficient, high-affinity interaction with PKR (Figure 2). Deletion of M1 results in the loss of efficient interaction with PKR and also in loss of apoptosis-inducing activity. Our studies also indicated that each of the three motifs individually was incapable of binding to PKR, further supporting our conclusion that two copies of the motif are required for efficient interaction with PKR. Deletion of the M3 motif resulted in a protein that retained its PKR-interaction ability to the full extent, but had lost its PKR-activating capacity completely. In fact, such a mutant resulted in inhibition of PKR activity both *in vivo* and *in vitro*. These results identify M1 and M2 as the PKR-interaction domains, and M3

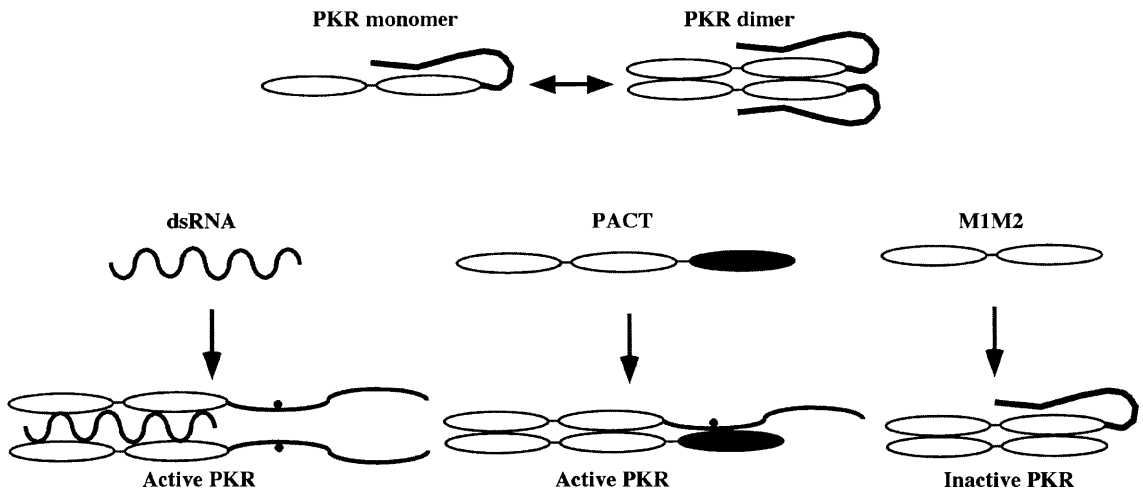

Figure 8 Model for PKR activation by PACT and inhibition by M1M2

PKR has two dsRNA-binding/protein interaction domains at its N-terminus, as depicted by the white ovals. The C-terminal kinase activity domains are folded such that the ATP-binding site is not exposed. PKR exists in equilibrium in monomeric and dimeric forms in the absence of its activator. Binding of dsRNA to the dsRNA-binding domains of PKR causes a conformational change in the molecules, leading to a stabilization of the dimeric form, and also exposes the ATP-binding site, which is indicated by a black circle. The two conserved dsRNA-binding/protein interaction domains of PACT are shown as white ovals and the third, less conserved, domain is shown as a black oval. PACT heterodimerizes with PKR through its protein-interaction domains, leading to a conformational change that also unmasks the ATP-binding site, resulting in the activation of PKR. The third domain of PACT interacts with a C-terminal domain of PKR in PKR's active conformation. M1M2, the deletion mutant of PACT, also can interact with PKR through its protein-interaction domains. However, this interaction does not lead to a favourable conformational change, due to the lack of domain M3, and therefore results in inhibition of PKR activity.

as the PKR-activation domain, of PACT. To test further if M3 is sufficient for PKR activation, we used purified recombinant M3 protein as an activator in PKR activity assays. Addition of M3 protein resulted in dose-dependent PKR activation, thereby confirming that M3 is both required and sufficient for activation of PKR. Similar to our results presented here, Peters et al. [49] reported recently that PACT's ability to activate PKR resides within the C-terminal M3 motif. Although our results are in general agreement with their observations, important differences emerge. These authors reported that a deletion construct of PACT lacking the M1 domain could efficiently activate PKR and induce apoptosis in HT1080 cells [49]. In our hands, deletion of motif M1 resulted in a total loss of PKR interaction, PKR activation and apoptosis-inducing capability. One difference between the two studies is the cell line used. We used NIH 3T3 cells in our transfection experiments; however, in our experience these differences are unlikely to cause such discrepancies. The differences could be attributed to the fact that our deletion construct lacked the N-terminal 126 amino acids, whereas the construct used by Peters et al. [49] lacked residues 36–99 but retained residues 1–35 and 99–126. This may result in different secondary structures of the two deletion products, leading to the observed differences. Alternatively, residues 1–35 or 99–126 may contribute to some extent to an efficient PACT–PKR interaction.

Although the M3 motif of PACT could activate PKR phosphorylation efficiently in a dose-dependent manner, at higher concentrations of M3 we noticed that, although the amount of PKR phosphorylation increased, the phosphorylation of eIF2α did not follow the same pattern. eIF2α phosphorylation showed an increase at lower concentrations of M3, which diminished when higher amounts of M3 were used. Further experiments revealed that the M3 domain of PACT and eIF2α compete for the same binding site on the PKR molecule. Residues mapping between amino acids 362 and 370 within PKR are known to be important for eIF2α binding [50,51]. Our data indicate that M3 interacts with PKR through residues downstream of position 318, thereby raising an interesting possibility that higher concentrations of M3 may be precluding the binding of eIF2α to PKR. This was further confirmed by the finding that co-immunoprecipitation of eIF2α with PKR could be competed out by M3. Native PACT, however, does not appear to behave similarly (results not shown), because the PACT–PKR interaction is driven mainly by the M1 and M2 motifs in PACT, and in such an interaction the M3 domain may interact very weakly or transiently within residues 318–551 of PKR to cause its activation.

Based on our results presented here, we can propose a model (Figure 8) for PKR activation by PACT. Latent PKR exists in equilibrium as monomeric and dimeric forms [37,55]. The conserved domain 2 of PKR is known to interact with its catalytic domain and inhibit its kinase activity [40,56]. Binding of dsRNA to the dsRNA-binding domain relieves the auto-inhibitory interaction between dsRNA-binding domains and catalytic domains, thereby facilitating activation. Binding of PKR to an activator has been shown to lead to a conformational change, unmasking the ATP-binding site and causing activation [4,56]. The interaction between PACT and PKR through the M1 and M2 motifs of PACT and the dsRNA-binding domain of PKR is predicted to result in a conformational change similar to the one brought about by dsRNA, exposing PKR's ATP-binding site. The third motif M3 of PACT interacts with a region within the catalytic domains of PKR, downstream of residue 318. This interaction of M3 with PKR is essential for PKR's activation, and deletion of M3 has an inhibitory effect on PKR activity, as shown on the extreme right of Figure 8. Interaction of M1M2 protein with PKR does not lead to a favourable conformational change due to the lack of M3, and this results in inhibition of PKR activity due to formation of inactive heterodimers between M1M2 and PKR.

The mechanism of the M3-mediated activation of PKR remains to be elucidated. We have shown previously that phosphorylation of PACT occurs rapidly in response to diverse stress signals, and this may lead to a more stable interaction between PKR and PACT [33]. The identity of the stress-activated kinase that phosphorylates PACT and the exact phosphorylation site remain to be determined. There are two possibilities for how phosphorylation of PACT could have an effect on PKR activation. One possibility is that PACT is phosphorylated within the M3 domain, and that this negatively charged phosphate is essential for PKR's activation following PACT–PKR association. In this case, phosphorylation of PACT would not be essential for an increased association between PACT and PKR, but would be a requisite for activation of PKR after the interaction. A second possibility is that PACT is phosphorylated on sites that are outside the M3 domain. It is possible that the PACT–PKR interaction is strengthened by the phosphorylation of PACT at residues outside the M3 domain, and that phosphorylation serves to increase the affinity between PKR and PACT. In the second scenario, phosphorylation of PACT would be essential for increased association and not for the actual activation process. Future experiments with PACT mutants are necessary to test these possibilities.

We thank Dr William Merrick for purified eIF2. This work was supported in part by grants K176 and E183 from Venture Fund/SC Educational Foundation and South Carolina Cancer Center respectively to R.C.P.

REFERENCES

1 Sen, G. C. and Ransohoff, R. M. (1993) Interferon-induced antiviral actions and their regulation. Adv. Virus Res. **42**, 57–102

2 Meurs, E., Chong, K., Galabru, J., Thomas, N. S., Kerr, I. M., Williams, B. R. and Hovanessian, A. G. (1990) Molecular cloning and characterization of the human double-stranded RNA-activated protein kinase induced by interferon. Cell **62**, 379–390

3 Clemens, M. J. and Elia, A. (1997) The double-stranded RNA-dependent protein kinase PKR: structure and function. J. Interferon Cytokine Res. **17**, 503–524

4 Hovanessian, A. G. and Galabru, J. (1987) The double-stranded RNA-dependent protein kinase is also activated by heparin. Eur. J. Biochem. **167**, 467–473

5 Samuel, C. E. (1993) The eIF-2α protein kinases, regulators of translation in eukaryotes from yeasts to humans. J. Biol. Chem. **268**, 7603–7606

6 Colthurst, D. R., Campbell, D. G. and Proud, C. G. (1987) Structure and regulation of eukaryotic initiation factor eIF-2. Sequence of the site in the alpha subunit phosphorylated by the haem-controlled repressor and by the double-stranded RNA-activated inhibitor. Eur. J. Biochem. **166**, 357–363

7 Katze, M. G. (1995) Regulation of the interferon-induced PKR: can viruses cope? Trends Microbiol. **3**, 75–78

8 Jagus, R., Joshi, B. and Barber, G. N. (1999) PKR, apoptosis and cancer. Int. J. Biochem. Cell Biol. **31**, 123–138

9 Williams, B. R. (1999) PKR; a sentinel kinase for cellular stress. Oncogene **18**, 6112–6120

10 Koromilas, A. E., Roy, S., Barber, G. N., Katze, M. G. and Sonenberg, N. (1992) Malignant transformation by a mutant of the IFN-inducible dsRNA-dependent protein kinase. Science **257**, 1685–1689

11 Meurs, E. F., Galabru, J., Barber, G. N., Katze, M. G. and Hovanessian, A. G. (1993) Tumor suppressor function of the interferon-induced double-stranded RNA-activated protein kinase. Proc. Natl. Acad. Sci. U.S.A. **90**, 232–236

12 Williams, B. R. G. (1995) The role of the dsRNA-activated kinase, PKR, in signal transduction. Semin. Virol. **6**, 191–202

13 Kumar, A., Yang, Y. L., Flati, V., Der, S., Kadereit, S., Deb, A., Haque, J., Reis, L., Weissmann, C. and Williams, B. R. (1997) Deficient cytokine signaling in mouse embryo fibroblasts with a targeted deletion in the PKR gene: role of IRF-1 and NF-kappaB. EMBO J. **16**, 406–416

14 Ramana, C. V., Grammatikakis, N., Chernov, M., Nguyen, H., Goh, K. C., Williams, B. R. and Stark, G. R. (2000) Regulation of c-myc expression by IFN-gamma through Stat1-dependent and -independent pathways. EMBO J. **19**, 263–272

15 Judware, R. and Petryshyn, R. (1991) Partial characterization of a cellular factor that regulates the double-stranded RNA-dependent eIF-2 alpha kinase in 3T3-F442A fibroblasts. Mol. Cell. Biol. **11**, 3259–3267

16 Salzberg, S., Mandelbaum, M., Zalcberg, M. and Shainberg, A. (1995) Interruption of myogenesis by transforming growth factor beta 1 or EGTA inhibits expression and activity of the myogenic-associated (2′-5′) oligoadenylate synthetase and PKR. Exp. Cell Res. **219**, 223–232

17 Lee, S. B. and Esteban, M. (1994) The interferon-induced double-stranded RNA-activated protein kinase induces apoptosis. Virology **199**, 491–496

18 Kibler, K. V., Shors, T., Perkins, K. B., Zeman, C. C., Banaszak, M. P., Biesterfeldt, J., Langland, J. O. and Jacobs, B. L. (1997) Double-stranded RNA is a trigger for apoptosis in vaccinia virus-infected cells. J. Virol. **71**, 1992–2003

19 Srivastava, S. P., Kumar, K. U. and Kaufman, R. J. (1998) Phosphorylation of eukaryotic translation initiation factor 2 mediates apoptosis in response to activation of the double-stranded RNA-dependent protein kinase. J. Biol. Chem. **273**, 2416–2423

20 Yeung, M. C., Liu, J. and Lau, A. S. (1996) An essential role for the interferon-inducible, double-stranded RNA-activated protein kinase PKR in the tumor necrosis factor-induced apoptosis in U937 cells. Proc. Natl. Acad. Sci. U.S.A. **93**, 12451–12455

21 Yeung, M. C. and Lau, A. S. (1998) Tumor suppressor p53 as a component of the tumor necrosis factor-induced, protein kinase PKR-mediated apoptotic pathway in human promonocytic U937 cells. J. Biol. Chem. **273**, 25198–25202

22 Der, S. D., Yang, Y. L., Weissmann, C. and Williams, B. R. (1997) A double-stranded RNA-activated protein kinase-dependent pathway mediating stress-induced apoptosis. Proc. Natl. Acad. Sci. U.S.A. **94**, 3279–3283

23 Gil, J., Alcami, J. and Esteban, M. (1999) Induction of apoptosis by double-stranded-RNA-dependent protein kinase (PKR) involves the alpha subunit of eukaryotic translation initiation factor 2 and NF-kappaB. Mol. Cell. Biol. **19**, 4653–4663

24 Gil, J., Alcami, J. and Esteban, M. (2000) Activation of NF-kappa B by the dsRNA-dependent protein kinase, PKR involves the I kappa B kinase complex. Oncogene **19**, 1369–1378

25 Balachandran, S., Kim, C. N., Yeh, W. C., Mak, T. W., Bhalla, K. and Barber, G. N. (1998) Activation of the dsRNA-dependent protein kinase, PKR, induces apoptosis through FADD-mediated death signaling. EMBO J. **17**, 6888–6902

26 Yeung, M. C., Chang, D. L., Camantigue, R. E. and Lau, A. S. (1999) Inhibitory role of the host apoptogenic gene PKR in the establishment of persistent infection by encephalomyocarditis virus in U937 cells. Proc. Natl. Acad. Sci. U.S.A. **96**, 11860–11865

27 Lee, S. B., Rodriguez, D., Rodriguez, J. R. and Esteban, M. (1997) The apoptosis pathway triggered by the interferon-induced protein kinase PKR requires the third basic domain, initiates upstream of Bcl-2, and involves ICE-like proteases. Virology **231**, 81–88

28 Cuddihy, A. R., Li, S., Tam, N. W., Wong, A. H., Taya, Y., Abraham, N., Bell, J. C. and Koromilas, A. E. (1999) Double-stranded-RNA-activated protein kinase PKR enhances transcriptional activation by tumor suppressor p53. Mol. Cell. Biol. **19**, 2475–2484

29 Goh, K. C., deVeer, M. J. and Williams, B. R. (2000) The protein kinase PKR is required for p38 MAPK activation and the innate immune response to bacterial endotoxin. EMBO J. **19**, 4292–4297

30 Bonnet, M. C., Weil, R., Dam, E., Hovanessian, A. G. and Meurs, E. F. (2000) PKR stimulates NF-kappaB irrespective of its kinase function by interacting with the IkappaB kinase complex. Mol. Cell. Biol. **20**, 4532–4542

31 Bandyopadhyay, S. K., de La Motte, C. A. and Williams, B. R. (2000) Induction of E-selectin expression by double-stranded RNA and TNF-alpha is attenuated in murine aortic endothelial cells derived from double-stranded RNA-activated kinase (PKR)-null mice. J. Immunol. **164**, 2077–2083

32 Patel, R. C. and Sen, G. C. (1998) PACT, a protein activator of the interferon-induced protein kinase, PKR. EMBO J. **17**, 4379–4390

33 Patel, C. V., Handy, I., Goldsmith, T. and Patel, R. C. (2000) PACT, a stress-modulated cellular activator of interferon-induced double-stranded RNA-activated protein kinase, PKR. J. Biol. Chem. **275**, 37993–37998

34 Ito, T., Yang, M. and May, W. S. (1999) RAX, a cellular activator for double-stranded RNA-dependent protein kinase during stress signaling. J. Biol. Chem. **274**, 15427–15432

35 Fierro-Monti, I. and Mathews, M. B. (2000) Proteins binding to duplexed RNA: one motif, multiple functions. Trends Biochem. Sci. **25**, 241–246

36 Cosentino, G. P., Venkatesan, S., Serluca, F. C., Green, S. R., Mathews, M. B. and Sonenberg, N. (1995) Double-stranded-RNA-dependent protein kinase and TAR RNA-binding protein form homo- and heterodimers in vivo. Proc. Natl. Acad. Sci. U.S.A. **92**, 9445–9449

37 Patel, R. C., Stanton, P., McMillan, N. M., Williams, B. R. and Sen, G. C. (1995) The interferon-inducible double-stranded RNA-activated protein kinase self-associates *in vitro* and *in vivo*. Proc. Natl. Acad. Sci. U.S.A. **92**, 8283–8287

38 Romano, P. R., Green, S. R., Barber, G. N., Mathews, M. B. and Hinnebusch, A. G. (1995) Structural requirements for double-stranded RNA binding, dimerization, and activation of the human eIF-2 alpha kinase DAI in Saccharomyces cerevisiae. Mol. Cell. Biol. **15**, 365–378
39 Patel, R. C., Stanton, P. and Sen, G. C. (1996) Specific mutations near the amino terminus of double-stranded RNA-dependent protein kinase (PKR) differentially affect its double-stranded RNA binding and dimerization properties. J. Biol. Chem. **271**, 25657–25663
40 Wu, S. and Kaufman, R. J. (1997) A model for the double-stranded RNA (dsRNA)-dependent dimerization and activation of the dsRNA-activated protein kinase PKR. J. Biol. Chem. **272**, 1291–1296
41 Patel, R. C. and Sen, G. C. (1998) Requirement of PKR dimerization mediated by specific hydrophobic residues for its activation by double-stranded RNA and its antigrowth effects in yeast. Mol. Cell. Biol. **18**, 7009–7019
42 St Johnston, D., Brown, N. H., Gall, J. G. and Jantsch, M. (1992) A conserved double-stranded RNA-binding domain. Proc. Natl. Acad. Sci. U.S.A. **89**, 10979–10983
43 Green, S. R. and Mathews, M. B. (1992) Two RNA-binding motifs in the double-stranded RNA-activated protein kinase, DAI. Genes Dev. **6**, 2478–2490
44 Tian, B. and Mathews, M. B. (2001) Functional characterization of and cooperation between the double-stranded RNA binding motifs of the protein kinase PKR. J. Biol. Chem. **276**, 9936–9940
45 Kaufman, R. J. and Murtha, P. (1987) Translational control mediated by eucaryotic initiation factor-2 is restricted to specific mRNAs in transfected cells. Mol. Cell. Biol. **7**, 1568–1571
46 Davies, M. V., Furtado, M., Hershey, J. W., Thimmappaya, B. and Kaufman, R. J. (1989) Complementation of adenovirus virus-associated RNA I gene deletion by expression of a mutant eukaryotic translation initiation factor. Proc. Natl. Acad. Sci. U.S.A. **86**, 9163–9167
47 Kaufman, R. J., Davies, M. V., Pathak, V. K. and Hershey, J. W. (1989) The phosphorylation state of eucaryotic initiation factor 2 alters translational efficiency of specific mRNAs. Mol. Cell. Biol. **9**, 946–958
48 Park, H., Davies, M. V., Langland, J. O., Chang, H. W., Nam, Y. S., Tartaglia, J., Paoletti, E., Jacobs, B. L., Kaufman, R. J. and Venkatesan, S. (1994) TAR RNA-binding protein is an inhibitor of the interferon-induced protein kinase PKR. Proc. Natl. Acad. Sci. U.S.A. **91**, 4713–4717
49 Peters, G. A., Hartmann, R., Qin, J. and Sen, G. C. (2001) Modular structure of PACT: distinct domains for binding and activating PKR. Mol. Cell. Biol. **21**, 1908–1920
50 Sharp, T. V., Witzel, J. E. and Jagus, R. (1997) Homologous regions of the alpha subunit of eukaryotic translational initiation factor 2 (eIF2alpha) and the vaccinia virus K3L gene product interact with the same domain within the dsRNA-activated protein kinase (PKR). Eur. J. Biochem. **250**, 85–91
51 Cai, R. and Williams, B. R. (1998) Mutations in the double-stranded RNA-activated protein kinase insert region that uncouple catalysis from eIF2alpha binding. J. Biol. Chem. **273**, 11274–11280
52 Gatignol, A., Buckler, W. A., Berkhout, B. and Jeang, K. T. (1991) Characterization of a human TAR RNA-binding protein that activates the HIV-1 LTR. Science **251**, 1597–1600
53 Gatignol, A., Buckler, C. and Jeang, K. T. (1993) Relatedness of an RNA-binding motif in human immunodeficiency virus type 1 TAR RNA-binding protein TRBP to human P1/dsl kinase and Drosophila staufen. Mol. Cell. Biol. **13**, 2193–2202
54 Benkirane, M., Neuveut, C., Chun, R. F., Smith, S. M., Samuel, C. E., Gatignol, A. and Jeang, K. T. (1997) Oncogenic potential of TAR RNA binding protein TRBP and its regulatory interaction with RNA-dependent protein kinase PKR. EMBO J. **16**, 611–624
55 Carpick, B. W., Graziano, V., Schneider, D., Maitra, R. K., Lee, X. and Williams, B. R. (1997) Characterization of the solution complex between the interferon-induced, double-stranded RNA-activated protein kinase and HIV-I trans-activating region RNA. J. Biol. Chem. **272**, 9510–9516
56 Nanduri, S., Rahman, F., Williams, B. R. and Qin, J. (2000) A dynamically tuned double-stranded RNA binding mechanism for the activation of antiviral kinase PKR. EMBO J. **19**, 5567–5574

Received 31 January 2002/16 April 2002; accepted 2 May 2002
Published as BJ Immediate Publication 2 May 2002, DOI 10.1042/BJ20020204